Normal Zone Propagation in High-Current Density Nb_3Sn Conductors for Accelerator Magnets

A. den Ouden, H. van Weeren, W. A. J. Wessel, H. H. J. ten Kate, G. A. Kirby, N. Siegel, and T. Taylor

***Abstract*—Self-absorbing quench protection schemes for accelerator magnets mainly rely on longitudinal and turn-to-turn normal zone propagation (NZP) immediately after the occurrence of a quench and subsequently on the effectiveness of protection heaters. Especially for impregnated Nb_3 Sn coils the protection should not only aim at limitation of the hot spot temperature and internal voltages but also at avoidance of large temperature gradients and local stress accumulation. Considering Rutherford types of cable based on present high current density Nb_3 Sn wires with a relatively low stabilizer content, a priori knowledge about their NZP properties is mandatory. Especially the medium and low-field properties appear to be critical for coil protection. The longitudinal NZP velocity of PIT-type Nb_3 Sn conductors are investigated both experimentally and numerically in nearly adiabatic conditions typical for impregnated coils. Numerical simulations are extended to extremely high current density Nb_3 Sn conductors and protection heater performance.**

***Index Terms*—Accelerator magnet, Nb_3 Sn superconductor, normal zone propagation, Rutherford cable.**

I. Introduction

QUENCH protection of high current density accelerator magnets relies on three decisive moments after an initially uncontrolled growth of a normal zone (NZ): $(\mathrm{t_d})$ detection of an expanding NZ as soon as the voltage generated by the NZ exceeds a certain threshold, $(\mathrm{t_{hf}})$ firing of the quench heaters and $(\mathrm{t_{he}})$ the moment the heaters become effective. Especially for fully impregnated Nb_3 Sn coils the protection should not only aim at limitation of the hot spot temperature and internal voltages but also at the avoidance of large temperature gradients and corresponding large stresses. Design of the essential protective elements (voltage threshold, heater lay-out, heater power, heater time constant, heater location in the coils etc.) are dictated by the local NZ propagation properties in the specific coil geometry. These in turn are a complex function of $I_c(B,T)$, the copper fraction, the (I_{op},B)-relation per conductor, the thermal properties $\rho(B,T)$ $\lambda(B,T)$ and $C(T)$ of the conductor and other cable constituents, the filling factor of the Rutherford cable and if applicable eventual cooling conditions or quench-back properties through the inter-strand resistances R_a and R_c. These properties have been extensively investigated for LHC related NbTi conductors, coil geometries and operating conditions, resulting in a nice set of numerical tools which are possibly applicable to Nb_3 Sn based elements too [1].

However, such basic information is lacking for Nb_3 Sn based conductors with a Cu:Sc ratio close to 1, operating in the medium field range from 10–15 T with a non-Cu current density ranging from 2000 to 3000 $\mathrm{A/mm^2}$. Therefore we have investigated above basic NZ propagation properties of a binary PIT-504 type of Nb_3 Sn conductor by determination of the NZ propagation velocity $\mathrm{v_{nz}}$, both experimentally and numerically. This conductor will be employed in an 88 mm bore, 10 T model dipole magnet [2]. The numerical simulations are extended to $(\mathrm{NbTa})_3$ Sn conductors with a non-Cu J_c larger than 2000 $\mathrm{A/mm^2}$ @ 12 T, relevant in present Nb_3 Sn accelerator magnet development. Finally, the numerical scheme appears to be a useful tool for heater design and performance verification.

II. Normal Zone Propagation

A. Numerical Modeling

To obtain a transparent, flexible, user friendly and relatively easily extendable numerical tool a quas-3D fully explicit finite difference scheme is developed to solve the well known heat equation which governs the thermal diffusion process of an expanding NZ for a set of adjacent cables equipped with quench heaters. Copper is assumed as the matrix material. The parameterized material properties λ, ρ and C of Cu(RRR), Nb, Nb_3 Sn, Sn, kapton, glass fiber-epoxy and glass/mica are temperature and, where applicable, field dependent [3]–[5]. Composite fractions of the PIT-conductor are estimated from cross sectional micro-graphs. Non-Cu $J_c(B,T)$-values of the specific Nb_3 Sn conductor, preferably based on actual $I_c(B,T)$ measurements, are calculated using the $J_c(B,T)$ scaling equations neglecting the strain dependency [6]. Output of the numerical scheme consists of temperature and voltage at desired time stamps and locations.

1) Heating During the Transition: Applicability of the concept of current sharing (CS) with a linear heating function, which works so well for NbTi, is not a priori justified for Nb_3 Sn [7]. This concept states that if the local conductor temperature T_{loc} lies between the current sharing temperature $T_{cs}(I_{op},B)$ (where I_{op} equals $I_c(B,T)$) and $T_c(B)$, the operating current I_{op} is shared between the superconductor and the copper matrix. Heat generation per unit length is described by the function G_{CS}:

$$G_{CS} = \begin{cases} \rho_m \frac{I_{op}^2}{A_m} \left(\frac{T-T_{cs}}{T_c-T_{cs}}\right) & T_{cs} < T < T_c \\ \rho_m \frac{I_{op}^2}{A_m} & T > T_c \end{cases} \quad (1)$$

Manuscript received October 20, 2003.

A. den Ouden, H. van Weeren, W. A. J. Wessel, and H. H. J. ten Kate are with the University of Twente, P.O. Box 217, NL 7500 AE Enschede, The Netherlands (e-mail: a.denouden@utwente.nl).

G. A. Kirby, N. Siegel, and T. Taylor are with CERN, CH 1211 Geneva 23, Switzerland (e-mail: g.a.kirby@cern.ch).

Digital Object Identifier 10.1109/TASC.2004.829082

in which ρ_m is the matrix resistivity and A_m the matrix cross-sectional area.

Instead, we have applied a more general concept of current sharing based on the $E-J$ relation during the transition, taking into account the normal state resistivity of the superconductor, which is not important for NbTi or Nb_3 Sn filaments in a Cu matrix but certainly for MgB_2 filaments in a Fe matrix. Assuming that the $E-J$ relation for the superconductor can be written as a power law,

$$E = E_0 \left(\frac{J_{sc}}{J_c}\right)^n. \tag{2}$$

we can rewrite the $E-J$ relation for the composite and compose a more general heating function G_{EJ} as:

$$I_{op} = \begin{cases} A_m \frac{E_{SC}}{\rho_m} + A_{sc}\left(J_C\left(\frac{E_{SC}}{E_C}\right)^{\frac{1}{n}}\right) & E_{SC} < E_{NC} \\ A_m \frac{E_{NC}}{\rho_m} + A_{sc}\frac{E_{NC}}{\rho_{sc}} & E_{SC} > E_{NC} \end{cases} \tag{3}$$

$$G_{EJ} = E_{SC,NC} I_{op}. \tag{4}$$

I_{op} is the total transport current through the conductor; E_{SC} is the electric field in the superconducting state; E_{NC} is the electrical field in the normal conducting state; J_c is the field and temperature dependent critical current density in the filaments (described by the Nb_3 Sn scaling relations), n is the field and temperature dependent n-value and E_c is the critical electrical field. For n-values above about 30, which is usually the case for these medium field, high J_c Nb_3 Sn conductors, G_{EJ} is not sensitive to the actual n-value anymore. Current sharing is expressed by the parallel circuit of the filaments and the matrix in two modes. First the superconducting mode, where the Nb_3 Sn filaments are still superconductive and E_{SC} is the resulting electric field. Secondly there is the normal conducting mode, where the Nb_3 Sn filaments and the matrix form a parallel circuit of two resistors over which the resulting electrical field is E_{NC}. Both E_{SC} and E_{NC} are continuously compared, so that the transition between the superconducting state and normal conducting state occurs when E_{SC} exceeds E_{NC}.

2) Multi-Element Modeling: To investigate turn-to-turn propagation, adjacent conductors can be connected to a NZ carrying conductor by insulating layers (in our case glass/mica and epoxy impregnated glass fibers). The most outer conductor is cooled by a 4.2 K heat sink with infinite capacity. Also quench heaters, modeled as stainless steel strips covering a required length of the conductor, can be connected to the conductors by an insulating layer consisting of glue, kapton and epoxy impregnated glass fibers. It is important to note that the heat capacity of these insulating layers, however thin, should not be neglected.

B. Experimental Set-Up

Measurements of the NZP velocity of Nb_3 Sn wire samples are performed under quasiadiabatic conditions using the insert depicted in Fig. 1. The insert is immersed into LHe and positioned in the bore of a 12 T magnet. Nb_3 Sn samples are heat treated on a standard TiAlV barrel, transferred to the cotton-

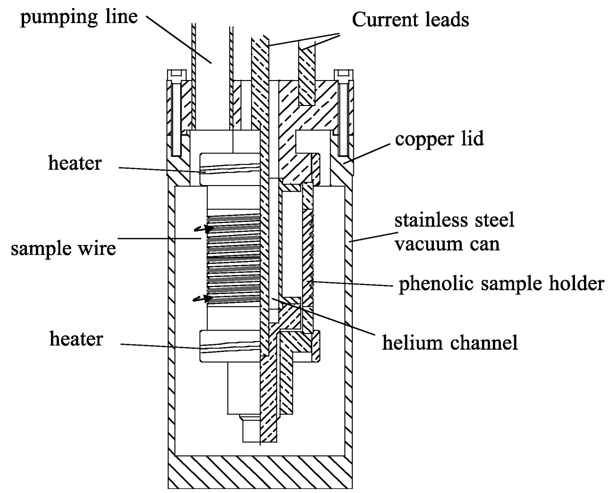

Fig. 1. Schematic lay-out of the sample holder for NZP measurements. The left hand side cutaway shows the sample holder, the right hand side the elements inside the sample holder.

phenolic (C-P) sample holder and finally soldered to the current leads. Sample fixation to the holder is achieved by a small amount of filled epoxy between the wire and the holder. This violates the adiabatic condition only slightly (see below). At a presently lowest temperature of (4.8 $+/-$ 0.1) K, mainly limited by the restricted cooling of the soldered lead connections inside the vacuum can, in fields up to 12 T and for currents up to 350 A the set-up allows measuring NZP properties of helical wire samples with a length of 1 meter. The temperature is regulated by a temperature controller, a thermometer mounted on the sample and two sample heaters located close to the soldering terminals.

NZP velocities are measured by the voltage time-of-flight method after applying a heat pulse with a wire wound heater. After the NZP measurements at 4.8 K, LHe is allowed into the vacuum chamber to enable a proper I_c measurement at 4.25 K in field. By applying the scaling equations for $I_c(B,T)$ the critical parameters at 4.8 K at the very same strain conditions of the particular sample are obtained with an estimated accuracy of about 2%.

We also measured the $I_c(4.2\ \mathrm{K})$ of a different sample of the same wire on a standard TiAlV sample holder. Taking into account the 0.12% difference in thermal contraction between the C-P and TiAlV sample holder, the obtained strain corrected $I_c(4.2\ \mathrm{K})$ agrees within a few percent with the independently measured I_c on the C-P sample holder.

III. Results and Discussion

A. Binary PIT- Nb_3 Sn

The investigated 0.9 mm PIT- Nb_3 Sn wire with 504 filaments exhibits a non-Cu J_c of 2200 $\mathrm{A/mm^2}$ at 10 T and 4.2 K, a cross sectional copper percentage of 55% and a RRR of 100. Fig. 2 shows the experimental and calculated normal zone propagation velocity as a function of the normalized transport current $(I/I_c(B))$ in a background field of 11 and 12 T at 4.8 K. Measured values are accurate within 5%. By adjusting only the heat capacity of the unknown residuals of the powder core in the filaments to reasonable values, satisfactory agreement between

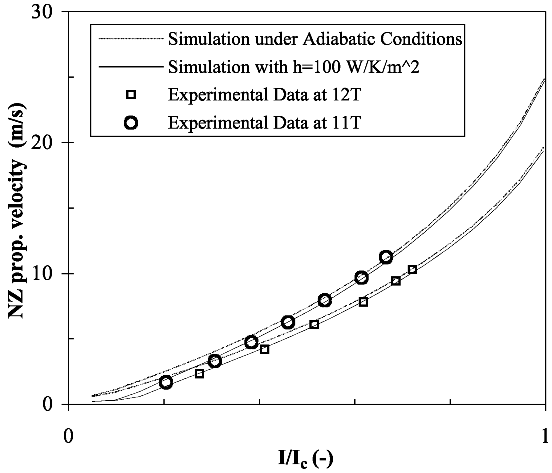

Fig. 2. Measured and calculated NZ propagation velocity v_{nz} of a binary Nb_3Sn conductor at 4.8 K in a background field of 11 and 12 T.

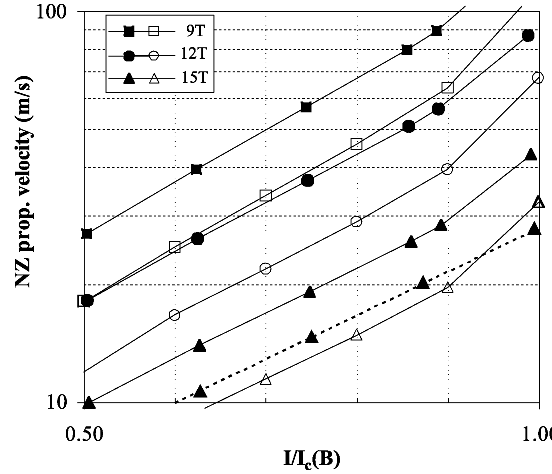

Fig. 3. Calculated v_{nz} of a $(NbTa)_3Sn$ conductor at 4.2 K with a non-Cu J_c at 12 T of 2 (open) and 3 kA/mm^2 (solid markers) as a function of $I/I_c(B)$. For comparison 15 T values using the G_{CS} function are included (dotted line).

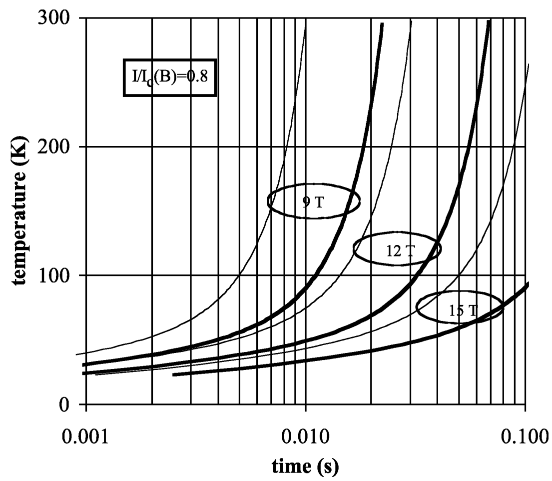

Fig. 4. Hot spot temperature evolution in time of a normal zone at several fields and $(I/I_c(BB)) = 0.8$ in a $(NbTa)_3Sn$ conductor with a non-Cu J_c at 12 T of 2 kA/mm^2 (bold lines) and 3 kA/mm^2 (thin lines).

measurements and simulations is obtained, especially at higher velocities where nonperfect adiabatic conditions become less dominant. Also shown are calculated values including cooling using a fitted parameter $\mathrm{h} = 100\ \mathrm{Wm^{-2}\,K^{-1}}$, which corresponds to a 0.2 mm thick glass/epoxy insulation layer with $\lambda(4.2\ \mathrm{K}) = 20\ \mathrm{mWm^{-1}\,K^{-1}}$.

The relatively low longitudinal NZP velocities are comparable to those measured for the pole face conductors of the MSUT dipole magnet. This is also the case for the turn-to-turn delay values in the range of 5–50 ms at 11 T over the current range of interest [9].

An important conclusion at this stage is that the good agreement between measurements and simulations validate the assumptions and parameters behind the numerical model and justify applicability of this scheme to a much wider (B,T,I)-range, also for Nb_3Sn conductors with a different composition.

B. High Current Density Ternary $(NbTa)_3Sn$

The numerical simulations have been extended to the most extreme performing $(NbTa)_3Sn$ wires developed by now, exhibiting a non-Cu J_c of 2–3 kA/mm^2 at 12 T and 4.2 K and a Cu-fraction of 47.5%. For comparison we use a PIT-lay-out with a RRR of 100. A lower RRR-value of 20–50 appears more realistic but only slightly affects the v_{nz}. For such a conductor Fig. 3 shows v_{nz} as a function of $(I/I_c(B))$ at several magnetic fields. To illustrate the difference between the classical CS-heating function (1) and the more appropriate EJ-heating function (4), also the 15 T values calculated with the G_{CS} function are included. This linearized G_{CS} underestimates significantly the v_{nz} over the whole current range, though at low $(I/I_c(B))$ the differences become small.

The hot spot temperatures for $(I/I_c(B)) = 0.8$ as a function of time are depicted in Fig. 4. If 300 K is the upper limit after quench detection and heater activation, it is clear that while taking advantage of their capacity, protection of coils employing such conductors is only possible at fields above 12 T or alternatively if the Cu-J_c remains below 1.8–2 kA/mm^2.

The heating function G_{EJ} described by (3) and (4) is more appropriate than a step function at T_{cs} from $G = 0$ to $G = 100\%$, used in recent FEM simulations of quenching Nb_3Sn coils [9]. This would result in an unrealistic overestimation of v_{nz} with at least a factor of 2 for $0.6 < (I/I_c) < 0.9$ at 12 T. Also application of Wilson's v_{nz}, using a step heating function evaluated at $0.5 * (T_{cs}(I,B) + T_c(B))$, overestimates v_{nz} by at least 30% in this field range [10].

C. Rutherford Cables and Protection Heaters

The twisted strands in a Rutherford cable usually experience rather steep field gradients in accelerator coils. For example, in the proposed 10 T dipole magnet, many inner layer conductors experience a maximum field of 10.3 T at the bore side but only 3 T at the outer radius of the layer. The impact on the NZ propagation is depicted in Fig. 5 which shows the temperature along a wire at time steps of 10 ms for a wire exposed to a longitudinally periodical field with a period of $\mathrm{L_p}$, an average field of 7 T and an amplitude of 3.5 T. Also shown are temperature profiles for a wire in a homogeneous field of 7 T. For both cases v_{nz} is rather similar, however, the hot spot temperature at the NZ origin is considerably higher in the periodical field case. Many simulations at different fields and field amplitudes confirm that

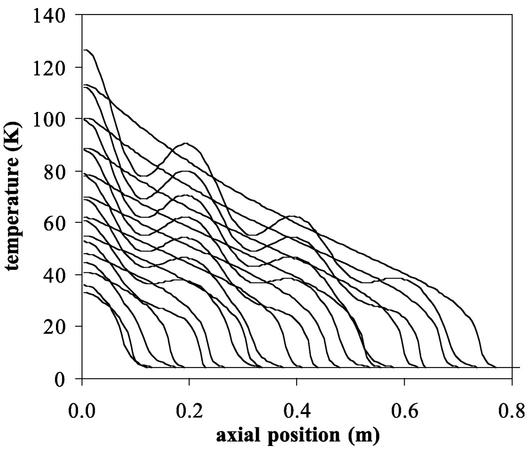

Fig. 5. Calculated temperature profile at time steps of 10 ms along a conductor that is exposed to a periodical field (bold lines) or to the corresponding average field (thin lines).

indeed the average field is a good approximation for the v_{nz} but definitely not for the hot-spot temperature.

We have also investigated the characteristics of fast responding LHC-type of quench heaters which consist of a 25 μm thick, 15 mm wide stainless steel strip periodically covered with copper, sandwiched between glue (22 μm), Kapton (75 μm) and glass fiber (50 μm). Such heaters should be co-impregnated with the coils to cover preferably both low-field and high-field conductors. For heater power densities ranging from 60–100 $\mathrm{Wcm^{-2}}$ with a time constant of 60 ms the temperature evolution of the covered part of the underlying conductor is calculated. The heaters become effective closely to $T_{cs}(I, B)$ which ranges in the proposed 10 T magnet from 7–14 K. With moderate heater power density all Nb_3Sn conductors are brought into transition at representative values of $T_{cs}(IB)$ within 30 ms, which at present is considered adequate for protection of this particular magnet which nominally operates at a maximum value of $(I/I_c(B))$ of 0.75.

IV. Conclusions

We have developed a fully explicit quasi 3D finite difference model to study stability and local normal zone properties in composite superconducting wires and conductor blocks. Also additional elements like protection heaters and surface cooling are optional features in the current model.

Agreement between calculations and measurements of the normal zone propagation velocity of a binary PIT- Nb_3Sn wire at representative fields and temperatures validate the assumptions and parameters underlying the numerical model, especially the more general approach of EJ-heating during the transition. Above justifies applicability of this scheme to a much wider (B,T,I)-range for both Nb_3Sn and MgB_2 conductors with different compositions.

The capabilities of the measuring set-up shall be adapted to a wider current and temperature range to enable an extended experimental verification of the numerical simulations.

With this numerical model all necessary basic input to verify the design parameters of a quench protection system for Nb_3Sn coils is quickly evaluated. This may prove to be a valuable tool to support more elaborate FEM methods to evaluate the quench process in full-size accelerator magnets.

References

[1] F. Sonneman and R. Schmidt, "Quench simulations for superconducting elements in the LHC accelerator," *Cryogenics 40*, pp. 519–529, 2000.

[2] A. den Ouden *et al.*, "Progress in the development of an 88 mm bore 10 T Nb_3Sn dipole magnet," *IEEE Trans. Appl. Supercond.*, vol. 11, no. 1, pp. 2268–2271, March 2001.

[3] G. R. Stewart and B. L. Brandt, "High-field specific heats of A15 V_3Si and Nb_3Sn," *Physical Review B*, vol. 29, no. 7, pp. 3908–3912, 1984.

[4] L. J. Vieland and A. W. Wicklund, "Specific heats of niobium-tin," *Physical Review*, vol. 166, no. 2, pp. 424–431, 1966.

[5] "Cryocomp is a Program That Computes Thermal Properties of Materials,", Copyright by Eckels Engineering, Florence, USA, distributed by Cryodata Inc..

[6] A. Godeke, B. ten Haken, and H. H. J. ten Kate, "Scaling of the critical current in ITER type niobium-tin superconductors in relation to applied field, temperature and uni-axial applied strain," *IEEE Trans. Appl. Supercond.*, vol. 9, no. 2, pp. 161–164, June 1999.

[7] J. Boschman, "On the Resistive Transition of Composite Super-Conductors," Ph.D. thesis, University of Twente, 1991.

[8] A. den Ouden, H. H. J. ten Kate, A. Siemko, P. Sievers, and L. Walckiers, "Quench characteristics of the 11 T Nb_3Sn model dipole magnet MSUT," in *Proceedings of 15th International Conference on Magnet Technology (MT15)*, Beijing, China, 1998, Science Press, pp. 339–342.

[9] S. Caspi, L. Chiesa, P. Feracin, S. A. Gourlay, R. Hafalia, R. Hinkins, A. F. Lietzke, and S. Prestemon, "Calculating quench propagation with ANSYS," *IEEE Trans. Appl. Supercond.*, vol. 13, no. 2, pp. 1714–1717, June 2003.

[10] M. N. Wilson, *Superconducting Magnets*, England: Oxford Science Publishing, 1983.